Development/Plasticity/Repair

Netrin Participates in the Development of Retinotectal Synaptic Connectivity by Modulating Axon Arborization and Synapse Formation in the Developing Brain

Colleen Manitt, Angeliki M. Nikolakopoulou, David R. Almario, Sarah A. Nguyen, and Susana Cohen-Cory
Department of Neurobiology and Behavior, University of California, Irvine, Irvine, California 92697

Netrin has been implicated in retinal ganglion cell (RGC) axon pathfinding in a number of species. In *Xenopus laevis*, RGC axons reaching their target in the optic tectum can be repelled by a netrin-1 gradient *in vitro*, suggesting that netrin may also function in wiring events that follow successful axon pathfinding. Here, we examined the contribution of netrin to RGC axon arborization and synapse formation at the target. Time-lapse confocal microscopy imaging of individual RGC axons coexpressing GFP-synaptobrevin and DsRed in the intact *Xenopus* brain demonstrated a role for deleted in colorectal cancer (DCC)-mediated netrin signaling. Microinjection of netrin-1 into the tectum induced a rapid and transient increase in presynaptic site addition that resulted in higher presynaptic site density over a 24 h observation period. Moreover, netrin induced dynamic axon branching, increasing branch addition and retraction; a behavior that ultimately increased total branch number. In contrast, microinjection of DCC function-blocking antibodies prevented the increase in presynaptic site number normally observed in control axons as well as the associated increase in branch number and axon arbor growth. Dynamic analysis of axon arbors demonstrated that the effects of anti-DCC on axon morphology and presynaptic connectivity were attributable to a specific decrease in new synapse and branch additions, without affecting the stability of existing synapses and branches. Together, these results indicate that, in the absence of DCC signaling, RGC axons fail to branch and differentiate, and support a novel role for netrin in later phases of retinotectal development.

Introduction

During neural network formation, growth cones at the leading edge of extending axons are required to make a series of pathfinding decisions to reach their final targets. Growth cone decisions are controlled by directional cues, either through contact-mediated mechanisms or presented as long-range gradients. Directional cues influence Rho GTPase function as well as other factors that impact on cytoskeletal dynamics that direct axon growth (Guan and Rao, 2003; Gallo and Letourneau, 2004; Govek et al., 2005). There are many intriguing similarities between the cytoskeletal dynamics involved in growth cone pathfinding and those involved in branching and synaptogenesis (Scheiffele, 2003; Kornack and Giger, 2005), suggesting that guidance factors can continue to participate in the organization of neuronal connectivity after pathfinding events have occurred. Indeed, an increasing number of studies now suggest that guidance cues contribute to plastic events that follow axon guidance to final targets (Dent et al., 2003; Kalil and Dent, 2005).

Received Feb. 25, 2009; revised June 19, 2009; accepted July 27, 2009.

This work was supported by National Eye Institute Grant EY011912. We thank Margarita Meynard and Justin Ling for help with multiple aspects of this project, and Dr. Cecilia Flores and members of our laboratory for helpful comments on this manuscript.

Correspondence should be addressed to either Colleen Manitt or Susana Cohen-Cory, Department of Neurobiology and Behavior, University of California, Irvine, 2205 McGaugh Hall, Irvine, CA 92697-4550, E-mail: colleen.manitt@mail.mcgill.ca or scohenco@uci.edu.

DOI:10.1523/JNEUROSCI.0947-09.2009

 0270-6474/09/2911065-13$15.00/0

Netrin-1 has been implicated in a number of neurodevelopmental events in addition to its well established role in axon guidance. Netrin-1 has been shown to influence axon branching in *Drosophila* and to modulate synaptogenesis in *Caenorhabditis elegans* (Winberg et al., 1998; Lim et al., 1999; Gitai et al., 2003; Colón-Ramos et al., 2007). Recent evidence demonstrating that netrin-1 induces axon back-branching in cortical neurons *in vitro* (Dent et al., 2004; Tang and Kalil, 2005), and that mature neurons in mice deficient in netrin receptor expression have fewer dendritic spines (Grant et al., 2007), suggests that netrin-1 is involved in the development of vertebrate synaptic connectivity as well.

In the developing visual system, netrin-1 can exert a bifunctional role in the guidance of retinal ganglion cell (RGC) axons to their brain targets. Netrin has been implicated in short-range guidance of RGC axons out of the retina in a number of species (Deiner et al., 1997; Höpker et al., 1999) and also guides axons further along the optic pathway (Mann et al., 2004). Evidence that *Xenopus* RGC axons about to enter their final target in the optic tectum respond to a gradient of netrin-1 *in vitro* (Shewan et al., 2002), suggests that netrin-1 may also function as a target recognition signal in the brain. Here, we have taken advantage of the *Xenopus laevis* visual system to observe dynamically, and *in vivo*, the contribution of netrin to the development of retinotectal synaptic connectivity by studying the morphological and synaptic differentiation of RGC arbors branching at their target.

Observations of actively branching axons in real time in frog and fish embryos have shown that branching and synaptogenesis are related events that impact on one another (Alsina et al., 2001;

Niell et al., 2004; Meyer and Smith, 2006). A limited number of *in vivo* time-lapse studies have examined the effects of specific cues on axon arbor differentiation (Cohen-Cory and Fraser, 1995; Cantallops et al., 2000; Campbell et al., 2007), which allow the distinction to be made between the ability of a cue to induce branch and synapse formation and its ability to influence their stability. Our findings identify deleted in colorectal cancer (DCC)-mediated netrin-1 signaling as a new key player in RGC axon branching and synaptogenesis in the vertebrate brain. Furthermore, our studies reveal axon dynamics that are unique to netrin signaling, suggesting that different cues may use specific dynamic strategies to influence the shape and function of developing neural circuits.

Materials and Methods

Animals. X. laevis tadpoles were obtained by *in vitro* fertilization of oocytes from adult females primed with human chorionic gonadotropin. Tadpoles were raised in 0.001% phenylthiocarbamide in rearing solution [60 mM NaCl, 0.67 mM KCl, 0.34 mM $Ca(NO_3)_2$, 0.83 mM $MgSO_4$, 10 mM HEPES, pH 7.4, 40 mg/L gentamycin] to prevent melanocyte pigmentation. Tadpoles were anesthetized in 0.05% tricane methanesulfonate (Finquel; Argent Laboratories) during experimental manipulations and were allowed to swim freely in rearing solution between imaging. Staging was according to Nieuwkoop and Faber (1956). Animal procedures were approved by the University of California, Irvine.

Antibodies and reagents. For immunohistochemical experiments, the following antibodies were used: an anti-chicken netrin-1 antibody raised against a sequence that is conserved in *X. laevis* (1:3500 dilution; Novus Biologicals) and an anti-human DCC antibody (1:1500 dilution; BD Biosciences Pharmingen). The specificity of the antibodies to recognize netrin and DCC, respectively, in *Xenopus* was tested by Western blot analysis (data not shown). A band of ~180 kDa was detected by the anti-DCC antibody in stage 38 retina, and a band of 75 kDa was detected by the netrin antibody in stage 45 tectum consistent with the predicted molecular weights of *Xenopus* DCC and netrin-1, and with previous reports (Pierceall et al., 1994). For colocalization studies, we also used antibodies against the presynaptic protein SNAP-25 (1:500 dilution; Assay Designs), the postsynaptic protein PSD-95 (mouse IgG; 1:200 dilution; Millipore), the microtubule associated protein microtubule-associated protein 2 (MAP2) (mouse IgG; 1:500 dilution; NeoMarkers), and an anti-neurofilament associated protein antibody (3A10; 1:2000 dilution). The 3A10 antibody developed by Dr. T. M. Jessell and Dr. J. Dodd (Columbia University, New York, NY) was used to immunostain presynaptic axon terminals and was obtained from the Developmental Studies Hybridoma Bank developed under the auspices of the National Institute of Child Health and Human Development and maintained by the Department of Biological Sciences of University of Iowa (Iowa City, IA). For imaging experiments, recombinant chicken netrin-1 (R&D Systems), anti-DCC function-blocking antibodies (AF5; Calbiochem) (Hong et al., 1999), and nonimmune mouse IgGs (Calbiochem) were used. The following expression plasmids were used for *in vivo* imaging studies: pDsRed express (Clontech) and GFP-synaptobrevin (a gift from Dr. M. M. Poo, University of California, Berkeley, Berkeley, CA) (Alsina et al., 2001).

Immunohistochemistry. Stage 45 *X. laevis* tadpoles were overdosed using tricaine methanesulfonate and fixed in 4% paraformaldehyde (PFA) in phosphate buffer (PB), pH 7.5, for 1 h. Brains were then dissected out and incubated overnight in 4% PFA at 4°C. Brains were embedded in 1% agarose and sectioned into 50 μm slices using a vibratome. DCC and netrin antigenicity were enhanced by gradually heating the free-floating sections to 95°C in PB. Sections were allowed to cool for 5 min and were then transferred to fresh PB. Tissue sections were incubated for 1 h at room temperature in blocking solution: 2% bovine serum albumin and 0.2% Tween 20 in PB. The sections were incubated with primary antibodies in blocking solution for 48 h at 4°C. For immunofluorescence analysis, primary antibodies were visualized using a donkey anti-mouse and anti-chicken, Alexa 488 and 568 secondary antibodies (Invitrogen; 1:500 dilution).

Preembedding immunoelectron microscopy. Stage 45 tadpoles were anesthetized and fixed in 2% paraformaldehyde, 3.75% acrolein in 0.1 M PB, pH 7.4. Brains were removed, postfixed, and embedded in 1% agarose. Fifty micrometer vibratome sections were collected, incubated in 1% sodium borohydride in PB, incubated in cryoprotectant for 30 min (25% sucrose and 3.5% glycerol in 0.05 M PB, pH 7.4), and quickly permeabilized in liquid nitrogen. Sections were blocked in 0.5% bovine serum albumin (BSA), 0.1 M Tris-buffered saline (TBS), and incubated with an anti-human DCC mouse antibody for 48 h (1:200 dilution in 0.1% BSA in TBS) at 4°C. Subsequently, the DCC antibody was detected by a goat anti-mouse IgG secondary antibody coupled to 1 nm gold particles for 2 h at room temperature (1:50 dilution in 0.5% v/v of 20% fish gelatin, 0.8% BSA in 0.01 M PBS, pH 7.4; Aurion-EMS). Sections were then incubated in 2% glutaraldehyde, and gold particles were enlarged using a British BioCell silver intensification kit (Ted Pella). The reaction was stopped by dipping the sections in 0.1 M TBS, pH 7.5. To control the occurrence of nonspecific labeling, adjacent sections were incubated without primary or secondary antibody alone in every experiment. The high specificity but low sensitivity of this preembedding immunostaining technique resulted in discrete silver precipitates of variable size in immunopositive axon terminals (because of enlargement of the 1 nm gold particles) (Rodríguez et al., 2005), which were absent in adjacent sections processed in the same manner but with the primary antibody being omitted in the incubation bath. Immunostained sections were postfixed in 2% osmium tetroxide, dehydrated, and flat embedded in 100% Epon. Using a stereoscope, the optic tectum was carefully dissected and placed on Epon blocks. Seventy nanometer thin sections were obtained on copper mesh grids using a Reichert ultramicrotome with a diamond knife (Diatome) and counterstained with 2% uranyl acetate and Reynolds lead citrate. Ultrastructural analysis was performed using a Philips CM10 transmission electron microscope.

GFP-synaptobrevin in vivo *expression and axon labeling.* The method used for the simultaneous visualization of axon arbor morphology and presynaptic sites in individual RGC axons *in vivo* was as described previously (Alsina et al., 2001). Briefly, a chimeric gene coding for wild-type green fluorescent protein (GFP) and the complete sequence of *X. laevis* synaptobrevin II was used to target GFP expression to synaptic vesicles in live tadpoles. Retinal progenitor cells of stage 20–24 tadpoles were cotransfected by lipofection (Holt et al., 1990) with equimolar amounts of GFP-synaptobrevin and pDsRedexpress (Clontech). Tadpoles were reared until stage 44, and then screened for axons coexpressing both expression plasmids. Only tadpoles with one to two axons colabeled were used for experimentation and imaging. Expression of GFP-synaptobrevin in RGC axons has been shown to highly colocalize with the expression of endogenous presynaptic and postsynaptic markers *in vivo* (95.8 ± 1.11% of the GFP-synaptobrevin puncta coincided with endogenous PSD-95; $n = 9$ brains, 262 GFP-labeled puncta, 5 independent experiments) (Alsina et al., 2001), to localize to truly recycling synaptic vesicles in *Xenopus* RGC axons *in vitro* (identified by stimulus-induced unloading of FM 4-64 dye) (Alsina et al., 2001), and is enriched at ultrastructurally mature RGC presynaptic terminals *in vivo* (Hu et al., 2005).

Time-lapse imaging. The behavior of individual RGC axons was followed with confocal microscopy in stage 44–45 tadpoles. Only tadpoles with individual RGC axons labeled with DsRed express showing specific, punctate GFP labeling in their terminals were selected. Tadpoles containing one or two clearly distinguishable double-labeled axons, with at least 20 branches were imaged every 4 h for 8 h, and then again at 24 h. Immediately after the first observation, 0.2–1.0 nl of recombinant chicken netrin-1 (300 ng/μl), anti-DCC (330 ng/μl), nonimmune mouse IgG (300 ng/μl), or vehicle solution (50% Niu Twitty) was pressure injected into the ventricle and subpial space overlying the optic tectum. Axon arbors in tadpoles injected with control, nonimmune IgG exhibited branch and GFP-synaptobrevin cluster dynamics comparable with those of vehicle-treated tadpoles (data not shown). To correlate GFP-synaptobrevin distribution with axon morphology, thin optical sections (1.5 μm) through the entire extent of the arbor were collected at 60× magnification (1.00 numerical aperture water-immersion objective) with a Nikon PCM2000 laser-scanning confocal microscope equipped

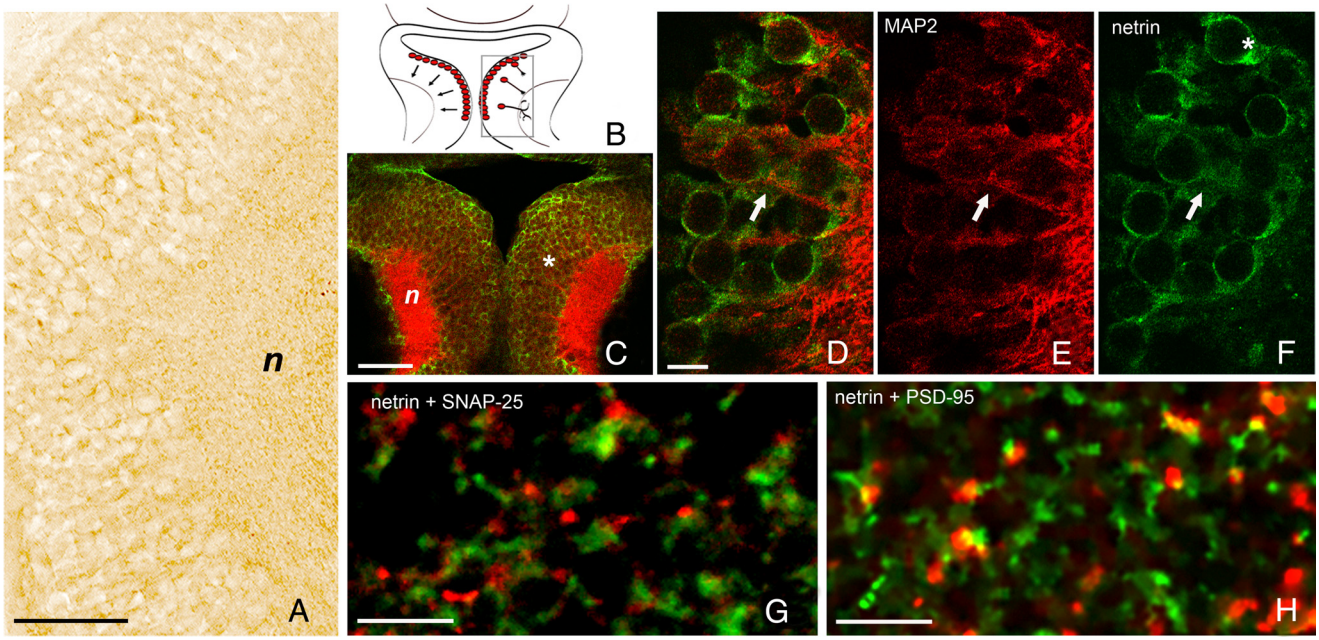

Figure 1. Netrin is present in tectal neurons and is identified at synaptic sites in the stage 44–45 *Xenopus* optic tectum. ***A***, ***B***, Localization of netrin immunoreactivity in the tectal midbrain. ***B***, Schematic diagram of a stage 44–45 *Xenopus* tectal midbrain (horizontal view). Neuronal precursors, born in rows adjacent to the ventricle in the right and left sides of the optic tectum, follow a lateral and rostral migratory path while extending a primary dendrite that will eventually terminate in the tectal neuropil and begin to elaborate a dendritic arbor. In this diagram, the boxed region corresponds to the micrograph shown in ***A***. ***A***, This horizontal view of the optic tectum demonstrates that a large, evenly distributed subset of cells is immunopositive for netrin-1. Punctate immunostaining is also observed throughout the tectal neuropil (*n*). ***C–F***, Confocal micrographs of a horizontal section through the stage 44–45 *Xenopus* optic tectum coimmunostained with antibodies to netrin (green immunofluorescence) and the dendritic marker MAP2 (red immunofluorescence). ***C***, Note that MAP2 immunostaining identifies optic tectal neuron dendritic processes projecting to and branching in the tectal neuropil (*n*). ***D–F***, The high-magnification confocal image reveals that netrin immunoreactivity is localized to cell bodies (asterisk) and proximal dendrites (arrow) of neurons within the medial portion of the optic tectum that are also immunoreactive for MAP2. ***G***, Confocal micrograph of the tectal neuropil in stage 44–45 *Xenopus* optic tectum coimmunostained with antibodies to netrin (red immunofluorescence) and the presynaptic marker SNAP-25 (green immunofluorescence). Note the punctate distribution of netrin (red) and SNAP-25 (green) in the tectal neuropil; the netrin-immunoreactive puncta are in direct apposition to SNAP-25-labeled presynaptic sites. ***H***, Confocal micrograph of stage 44–45 *Xenopus* optic tectum coimmunostained with antibodies to netrin (red immunofluorescence) and the postsynaptic marker, PSD-95 (green immunofluorescence). Netrin-immunoreactive puncta in the tectal neuropil colabel with PSD-95-positive postsynaptic densities. Scale bars: ***A***, 50 μm; ***C***, 100 μm; ***D–F***, 10 μm; ***G***, ***H***, 5 μm.

with argon (488 nm excitation; 10% neutral density filter) and HeNe (543 nm excitation) lasers. A 515/30 nm (barrier) emission filter and a 605/32 nm (bandpass) emission filter were used for GFP-synaptobrevin and DsRed visualization, respectively. GFP-synaptobrevin and DsRed confocal images were obtained simultaneously, below saturation levels, with minimal gain and contrast enhancement.

Data analysis. All analysis was performed from raw confocal images without any postacquisition manipulation or thresholding as described previously (Alsina et al., 2001; Hu et al., 2005; Marshak et al., 2007). Analysis was performed blind to the treatment group. Digital three-dimensional reconstructions of GFP-synaptobrevin and DsRed-labeled arbors were obtained from individual optical sections through the entire extent of the arbor with the aid of the MetaMorph software (Molecular Devices). Presynaptic GFP-synaptobrevin clusters were characterized and measured from pixel-by-pixel overlaps from individual optical sections obtained at the two wavelengths. In brief, yellow regions of complete red and green overlap of 0.5–1.0 μm^2 in size and 150–255 pixel intensity values were identified as GFP-synaptobrevin-labeled puncta. Individual GFP-synaptobrevin puncta were mapped on tracings derived from the entire three-dimensionally reconstructed axon arbor, and axon branches and puncta were marked, identified, and followed from one time point to the next. Several morphological landmarks (branch shape, bends, and swells) that remained stable across time points for each individual arbor allowed us to identify stable, added, and eliminated GFP-synaptobrevin puncta and branches from one observation time point to the next. Imaging of RGC axon terminals in the *Xenopus* brain *in vivo* at 5 min intervals for a period of 30–60 min demonstrated that GFP-synaptobrevin puncta characterized as above are not motile (B. Alsina, B. Hu, and S. Cohen-Cory, unpublished observations). To obtain a detailed analysis of presynaptic cluster dynamics at each observation interval, several parameters were measured: the location of each synaptic cluster along the axon arbor, the number of clusters per branch or per unit arbor length, the number of clusters added or eliminated, and the number of clusters maintained from one observation interval to the next. For the quantitative analysis of axon branching, total arbor branch length (length of total branches), total branch number, the number of individual branches gained or lost, and the number of branches remaining from one observation interval to the next were measured. To differentiate between nascent filopodia and branches, extensions from the main axon of >5 μm were classified as branches (Cohen-Cory and Fraser, 1995; Alsina et al., 2001; Hu et al., 2005; Marshak et al., 2007). A total of 17 axons for control, 14 for netrin, and 12 for anti-DCC treatment were analyzed, with one axon analyzed per tadpole. Axons analyzed had between 20–60 branches and 25–98 clusters. Data are presented both as net and percentage change from the initial value for each individual axon, or as the change between two observation intervals for every individual axon. Two-sample unpaired *t* tests were used for the statistical analysis of data. Results were classified as significant if $p \leq 0.05$.

Results

The spatial and temporal distribution of netrin and DCC receptor expression supports a role for netrin in retinotectal circuit development

The distribution of netrin was examined in the *Xenopus* optic tectum at stage 44–45, a developmental time point when retinal axons have terminated in the optic tectum and are actively branching and forming synapses with their postsynaptic partners, the tectal neurons. Tectal neurons are born in a row along the caudomedial border of the right and left tectum immediately adjacent to the ventricle (Fig. 1*A*,*B*). Tectal neuron cell bodies then migrate laterally and rostrally while extending their primary

dendrite toward the tectal neuropil in which they will branch and form connections with RGC axons. Netrin immunoreactivity was localized to a large subset of cell bodies in the optic tectum (Fig. 1*A*, *C*). Coimmunostaining of netrin-1 with MAP2, a dendritic marker, indicates that the netrin-immunoreactive cells in the optic tectum are neurons, with immunoreactivity being predominantly localized to neuronal cell bodies and occasional proximal dendrites (Fig. 1*C–F*). Within the tectal neuropil, large netrin-1-immunoreactive puncta were dispersed throughout, with the highest density of puncta being present in the rostral tectum, in the region of the neuropil directly adjacent to the tectal cell body layer (Fig. 1*A*) (also Fig. 2*F*, *H*, *I*). This highly immunoreactive area of the rostral tectum is densely populated by tectal dendrites because of its proximity to the cell body layer, and contains dendritic arbors from more mature tectal neurons. Thus, many branching RGC axons are making synaptic contacts with their postsynaptic partners within this region. The close apposition between netrin immunoreactivity and SNAP-25-immunoreactive puncta within the tectal neuropil (Fig. 1*G*) suggests that netrin is expressed by tectal neurons and is enriched near or at postsynaptic sites. Consistent with this, netrin-immunoreactive puncta colocalized with the endogenous postsynaptic density marker PSD-95 within the tectal neuropil (Fig. 1*H*).

The expression of the netrin-1 receptor, DCC, by RGCs has been reported previously at earlier stages of retinotectal development (de la Torre et al., 1997). We examined DCC mRNA and protein expression at stage 44–45 to confirm its presence on RGC axons actively branching in their target. *In situ* hybridization for DCC identified a number of neuronal subtypes, including RGCs, that express DCC within the retina at this developmental stage (data not shown), in a pattern consistent with that of previous reports (de la Torre et al., 1997). Immunostaining with antibodies to DCC showed that axonal fibers that project to the tectal neuropil express DCC (Fig. 2*B–I*). To confirm that these DCC-positive fibers correspond, at least in part, to RGC axons, we performed a unilateral eye ablation in young tadpoles. Sections of stage 45 tadpole optic tectum were immunostained with antibodies to DCC and 3A10, a marker for RGC axons (Fig. 2*B–E*). The distribution of 3A10 immunoreactivity in the ipsilateral and contralateral side of the optic tectum confirmed the absence of axon fiber bundles in the contralateral side of the optic tectum that would normally receive innervation from the ablated eye (Fig. 2*B*). Other populations of axons remained labeled with 3A10 indicating the location of other subpopulations of fibers in the same brain section (Fig. 2*B*). DCC immunostaining was abolished on the side of the optic tectum contralateral to the eye ablation along with that of 3A10, indicating that fibers positive for DCC were indeed RGC axons. The distribution of DCC-positive RGC axons in the unaffected side of the optic tectum, ipsilateral to the eye ablation, was compared with the entire 3A10-positive retinal axon bundle. Comparison of the two patterns of immunoreactivity thus indicated that a large subset of retinal axons is positive for DCC (Fig. 2*C*,*E*).

Sections obtained from stage 45 optic tectum were also double-labeled with antibodies to netrin and DCC to determine the relationship between the distribution patterns of the ligand and its receptor in the tectal neuropil (Fig. 2*F–I*). DCC immunoreactivity was present in RGC axon bundles and in arbors that had begun to branch. The two distribution patterns were clearly complementary (Fig. 2*F–H*), with the two labels in the neuropil being present in close apposition to each other (Fig. 2*I*). Consistent with the eye ablation experiments, another distinct population of fibers located more medially was also DCC positive (Fig. 2*E*, *G*). *In situ* hybridization experiments for DCC in the midbrain indicate that there is a ventral–dorsal graded distribution of DCC expression in this brain region at stage 44–45 (data not shown). The optic tectum, which is in the dorsal third of the midbrain, contained weak labeling indicating that there is very little or no DCC expression by tectal neurons in this area.

The subcellular distribution of DCC in the tectal neuropil was examined by preembedding, silver enhanced immunoelectron microscopy (see Materials and Methods). DCC immunoreactivity was found to be present at presynaptic specializations, both on presynaptic vesicles (Fig. 2*J*, *K*) and on the surface of presynaptic membranes (Fig. 2*L*). DCC immunoreactivity was also found on the surface of filopodia (Fig. 2*M*), and along the axon shaft (data not shown). This subcellular distribution of DCC immunoreactivity in presynaptic terminals thus supports a role for DCC-mediated netrin signaling in axon branching and synaptogenesis in the target optic tectum.

UNC-5 is a second netrin-1 receptor that has been associated with growth cone repulsive responses (Hedgecock et al., 1990; Keleman and Dickson, 2001; Finger et al., 2002). A pan-UNC-5 antibody (Tong et al., 2001; Manitt et al., 2004) was used to examine expression of UNC-5 in stage 45 *Xenopus* tadpoles. Consistent with previous reports (Anderson and Holt, 2002), UNC-5 immunoreactivity was absent from axon terminals of RGCs at this stage (data not shown). Thus, RGC axon terminals express DCC receptors as they enter and branch in the optic tectum, but are devoid of UNC-5.

Alterations in netrin signaling result in changes in RGC axon morphology and presynaptic site number

Once in the target optic tectum, RGC axon arbors become morphologically more complex by the dynamic addition, elimination, and stabilization of presynaptic sites and axon branches (O'Rourke and Fraser, 1990; Cline, 1991; Cohen-Cory and Fraser, 1995). In the following experiments, actively branching RGC axons were observed over a 24 h period after manipulations that alter netrin signaling. To visualize RGC arbors, stage 22 *Xenopus* embryos were lipofected in one eye with DsRed (red; entire axonal arbor) and GFP-synaptobrevin (green; presynaptic sites) (see Materials and Methods) (Alsina et al., 2001; Hu et al., 2005) expression vectors. At stage 44–45, tadpoles were screened and those with one to two axons coexpressing both plasmids were selected for time-lapse experiments. Axons ranging from 20 to 60 branches at the 0 h time point (time 0 h) were selected for statistical analyses. The mean number of branches or synapses across groups at "time 0 h" was not significantly different, nor was there any significant difference in axon arbor length (data not shown).

Microinjection of either vehicle or nonimmune mouse IgGs did not significantly affect any of the parameters measured relative to controls (see Materials and Methods). Microinjection of recombinant netrin-1, however, resulted in changes in axon arbor morphology and in the number GFP-synaptobrevin presynaptic sites (Figs. 3, 4). The change in the absolute number of labeled presynaptic sites relative to time 0 h was four times higher in the netrin-treated tadpoles by the first 4 h time point compared with controls (0–4 h, 10.27 ± 5.895 for control and 40.18 ± 5.838 for netrin treated; $p = 0.0018$) (Fig. 3*B*). A greater increase in the absolute number of GFP-synaptobrevin presynaptic sites was also observed 8 and 24 h after microinjection of recombinant netrin-1 (0–8 h, 21.47 ± 5.857 for control and 55.09 ± 6.408 for netrin treated, $p = 0.0008$; 0–24 h, 46.53 ± 8.129 for control and 106.2 ± 11.89 for netrin treated, $p = 0.0003$) (Fig. 3*B*), indicating

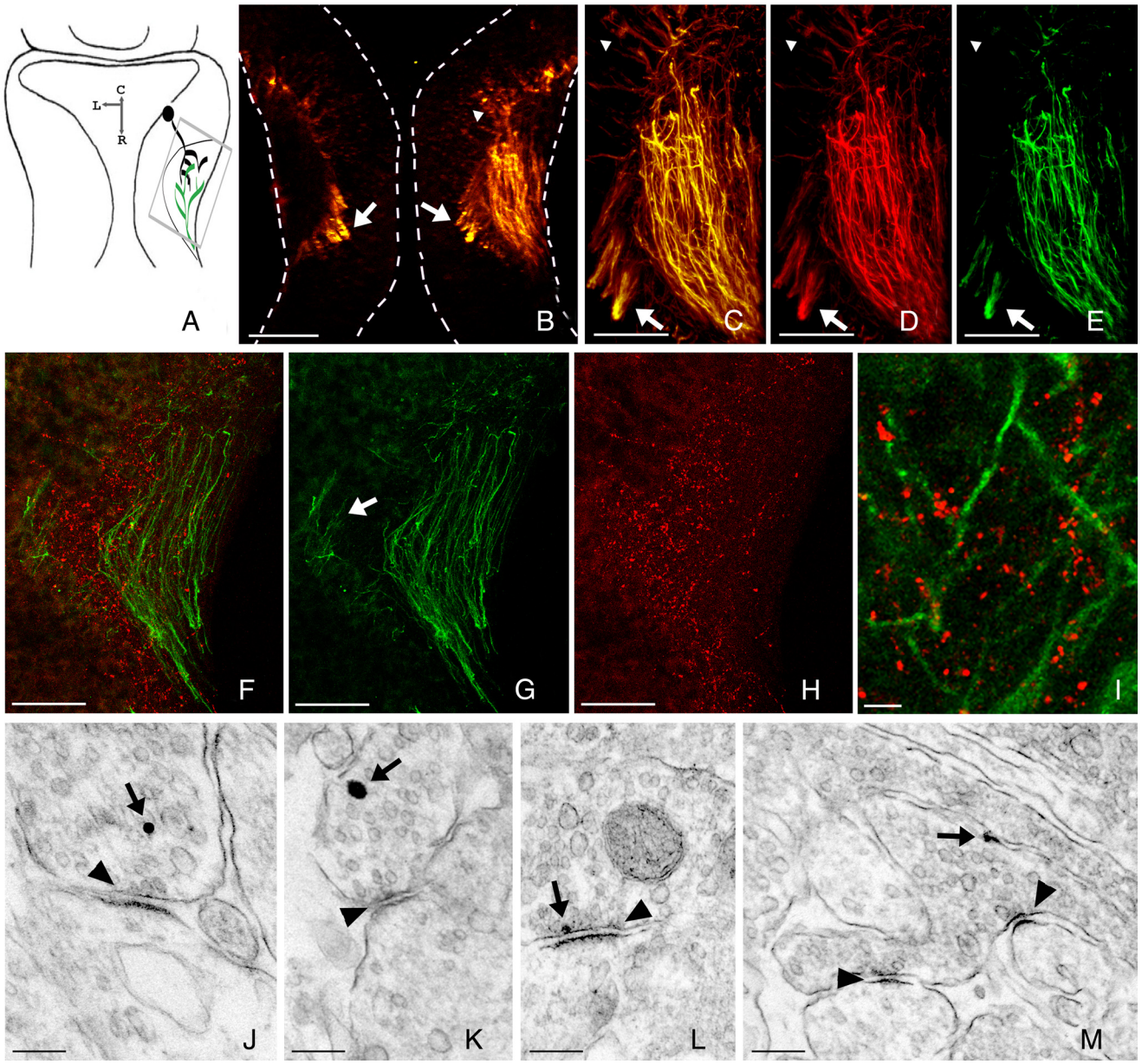

Figure 2. RGC axons branching the optic tectum are immunopositive for DCC at presynaptic sites. ***A***, Schematic illustration of the retinotectal circuit in stage 44–45 *Xenopus* optic tectum (horizontal view). RGC axons project to the neuropil in the lateral tectum, in which they elaborate an arbor and form synapses with tectal neuron dendrites. Confocal micrographs of the tectal neuropil shown in ***C–H*** correspond to regions demarcated by the gray box. ***B–E***, After unilateral right eye ablation, sections through the tectal midbrain were coimmunostained with antibodies to DCC and a marker for RGC axons (neurofilament-associated protein, 3A10). ***B***, Horizontal section showing the localization of 3A10 (red)- and DCC (green)-immunoreactive fiber bundles in the two sides of the tectal neuropil. A large bundle of double-labeled fibers in the right side of the optic tectum is absent from the left side, which normally would receive innervation from the right, ablated eye. This manipulation identifies the missing axonal fibers as RGC axons. Note that a smaller, more medial population of DCC-positive fibers remains intact after eye ablation (***B–E***, ***G***, arrows), indicating the presence of a distinct population of DCC-positive fibers in addition to RGCs. ***C–E***, High-power micrographs of the RGC axon bundle shown in ***B*** illustrates the colocalization of DCC (green) and 3A10 (red) immunoreactivities in the axonal fibers [double labeling (***C***); 3A10 immunoreactivity alone (***D***); DCC labeling alone (***E***)]. A high degree of colocalization in DCC and 3A10 immunoreactivity in RGC axons is observed. Note, however, that a small subset of cell bodies and their dendrites are also positive for 3A10 but negative for DCC (***B–E***, small arrowheads). ***F–I***, Micrographs of stage 44–45 *Xenopus* tectal neuropil coimmunostained with antibodies to DCC and netrin. DCC immunoreactivity (green) localizes to RGC axonal fibers projecting and branching in the tectal neuropil. Netrin immunoreactivity (red) is distributed in a punctate pattern in the tectal neuropil, in close proximity to DCC-positive axon fibers. ***I***, Higher power micrograph of the horizontal section shown in ***F*** better illustrates how the netrin-immunoreactive puncta (red) are in close apposition to DCC-positive fibers (green). ***J–M***, The subcellular localization of DCC in stage 44–45 optic tectum was determined by preembedding immunoelectron microscopy. The silver enhancement of secondary antibody-conjugated 1 nm gold particles shows that DCC immunoreactivity localizes to vesicles at presynaptic specializations (***J***, ***K***, arrows), as well as presynaptic membranes (***L***, arrow) in the tectal neuropil. The presence of a synapse is indicated by the arrowheads. ***M***, Discrete silver-enhanced DCC-immunoreactive clusters were also observed on presynaptic filopodia (arrow). Scale bars: ***B***, 100 μm; ***C–E***, 50 μm; ***I***, 5 μm; ***J***, ***K***, 0.2 μm.

that the elevated number of presynaptic clusters in the netrin-treated tadpoles relative to controls was maintained during the entire 24 h observation period.

Microinjection of recombinant netrin-1 also increased the total number of branches within the axon arbor over the 24 h observation period. The increase in absolute branch number relative to time 0 h in the netrin-treated tadpoles was three times higher than controls by the 8 h observation time point (0–8 h, 3.4 ± 1.253 for control and 10.93 ± 3.082 for netrin treated; $p = 0.0281$) and remained elevated at the final 24 h observation time

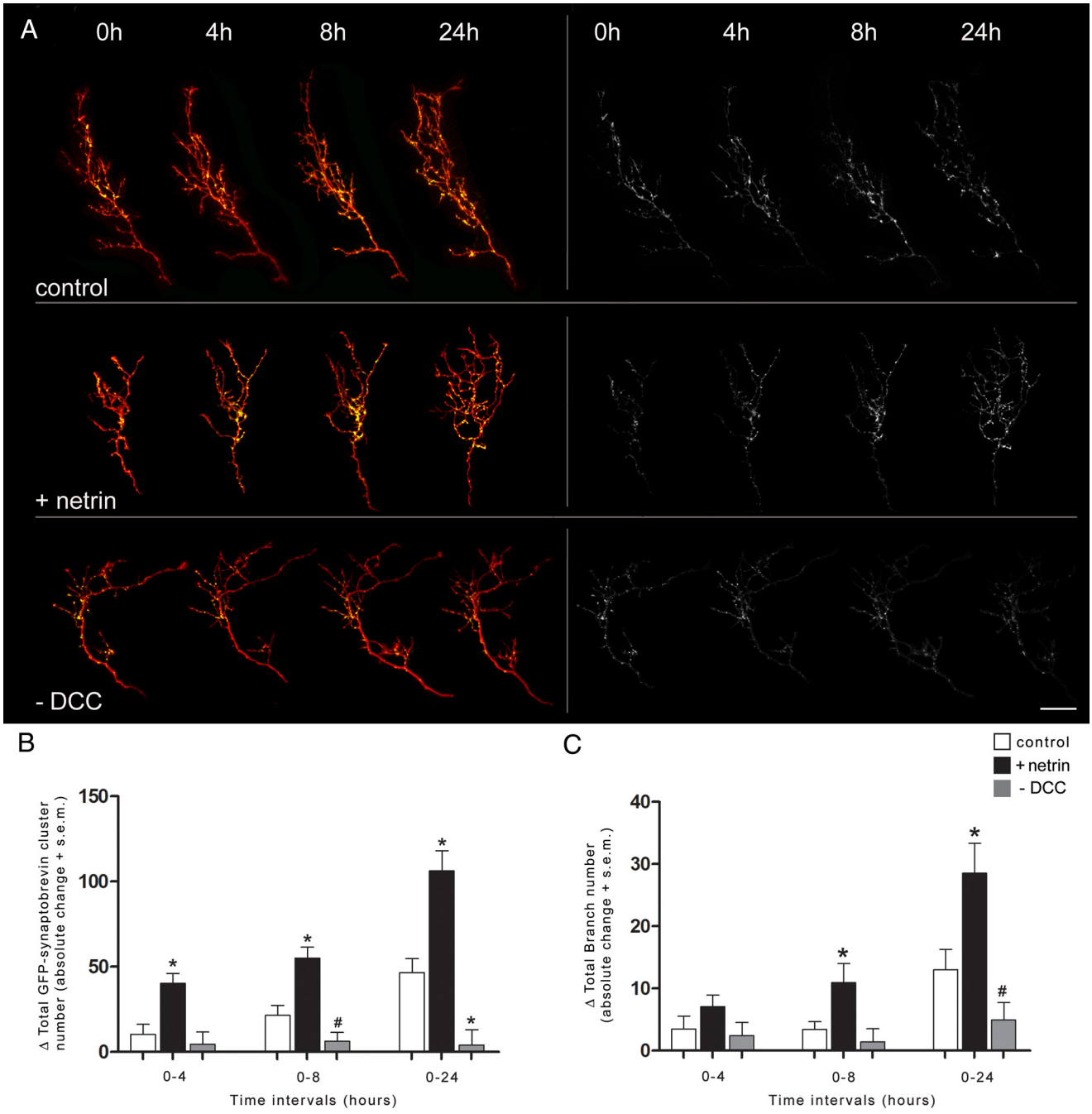

Figure 3. DCC-mediated netrin signaling contributes to RGC axon presynaptic differentiation during the development of retinotectal connectivity. ***A***, Sample RGC axons coexpressing Ds-Red (red) and GFP-synaptobrevin (green) imaged by time-lapse confocal microscopy over a 24 h period after microinjection of recombinant netrin-1 (+ netrin) or function-blocking antibodies to DCC (− DCC). Projections on the right show the GFP-synaptobrevin fluorescence only. Scale bar, 50 μm. ***B***, ***C***, Manipulations in netrin signaling alter the number of GFP-synaptobrevin-labeled presynaptic sites and influence RGC axon arbor morphology. ***B***, As RGC axons branch and differentiate, the absolute number of GFP-synaptobrevin-labeled presynaptic sites increases over time (0–4, 0–8, 0–24 h). Microinjection of recombinant netrin-1 induced a significantly higher increase in the number of presynaptic sites relative to controls by 4 h, an effect that persisted for the remainder of the 24 h observation period. Microinjection of DCC function-blocking antibodies led to a smaller increase in presynaptic site number relative to controls from 8 h onward. ***C***, The increase in the number of total branches was significantly higher in RGC axons 8 h after netrin treatment relative to controls, whereas RGC axons had fewer branches 24 h after anti-DCC treatment. *Significance with $p \leq 0.05$. #Trend toward significance with $0.05 > p < 0.10$. Error bars indicate SEM.

point (0–24 h, 13.00 ± 3.299 for control and 28.5 ± 4.845 for netrin treated; $p = 0.0125$) (Fig. 3*C*).

The impact of these changes relative to the entire axon arbor was examined by determining the percentage change in total branch or presynaptic site number at 4, 8, and 24 h relative to time 0 h for each individual axon. This measure of relative change in total presynaptic site and total branch number indicated that netrin-treated axons became synaptically and morphologically more complex. Netrin-treated RGC axons underwent a ~70% increase in presynaptic site number by 4 h compared with a ~20% increase in controls. This effect was maintained for the remainder of the 24 h observation period (0–4 h, 117.4 ± 7.81% for control and 166.4 ± 12.96% for netrin treated, $p = 0.0022$; 0–8 h, 139 ± 9.53% for control and 185.6 ± 11.78% for netrin treated, $p = 0.0053$; 0–24 h, 193.8 ± 18.74% for control and 264.5 ± 19.50% for netrin treated, $p = 0.0188$) (Fig. 4*A*). In

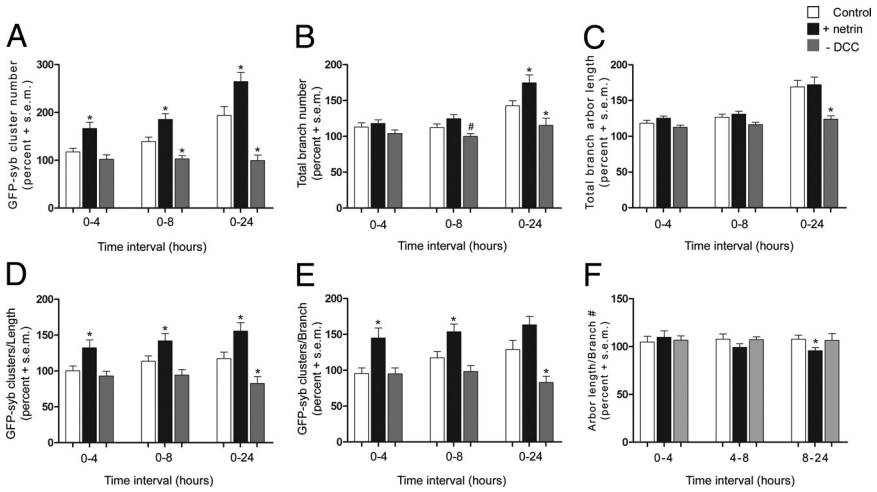

Figure 4. DCC-mediated netrin signaling contributes to RGC axon presynaptic differentiation during the development of retinotectal connectivity. Changes in RGC presynaptic differentiation and in axon arborization were measured and expressed as percentage of initial values for each individual axon. ***A***, Microinjection of recombinant netrin-1 into the optic tectum induced a significant increase in GFP-synaptobrevin-labeled presynaptic sites when compared with controls over a 24 h observation period. In contrast, microinjection of DCC function-blocking antibodies prevented the normal increase in presynaptic site number observed in controls over the 24 h observation period. ***B***, Even though netrin induces a significant net increase in branches 8 h after treatment (Fig. 3*C*), the increase in branch number in RGC axons in netrin-treated tadpoles relative to the initial branch number was significantly different from controls by 24 h only. In contrast, anti-DCC treatment prevented the increase in branch number observed in controls at 8 and 24 h. ***C***, The effect of anti-DCC treatment on axon arbor growth is also demonstrated by measuring the change in total arbor branch length. Total arbor branch length in RGC axons increased by 24 h in both control and netrin-treated tadpoles, whereas this measure was unchanged in the anti-DCC-treated tadpoles. ***D***, ***E***, The number of GFP-synaptobrevin-labeled presynaptic sites per unit arbor length and per branch number provided a measure of presynaptic site density. Netrin treatment significantly increased presynaptic site density in RGC axons from 4 h onward, whereas anti-DCC treatment resulted in RGC axons with lower presynaptic site density relative to controls by 24 h. ***F***, We obtained a comparative measure of branch length by calculating average axon segment length (length/branch) at each observation interval and expressing it as percentage of initial value for each axon. This measure revealed that, on average, axon branch segments in RGC axon arbors in netrin-treated tadpoles became shorter than controls from 8 to 24 h after treatment. *Significance with $p \leq 0.05$. #Trend toward significance with $0.05 > p < 0.10$. Error bars indicate SEM.

addition to its effects on presynaptic site number, netrin elicited a significant increase in total branch number by the end of the 24 h observation period (0–24 h, 142.5 ± 7.27% for control and 174.5 ± 11.19% for netrin treated; $p = 0.0198$) (Fig. 4*B*). Netrin-treated axons increased their branch number ~75% by 24 h, whereas controls increased their total branches by ~35% (Fig. 4*B*). Total axon branch length (Fig. 4*C*), and the areal extent of the axon arbor (supplemental Fig. 1, available at www.jneurosci.org as supplemental material), however, were not significantly different from controls, indicating that the changes in synapse and branch number were not simply attributable to an increase in the overall growth of the axon. Consistent with this, the increase in GFP-synaptobrevin-labeled presynaptic site number reflected a significant increase in presynaptic density (GFP-syb clusters/length, 0–4 h, 100.3 ± 6.54% for control, 132.2 ± 11.17% for netrin treated, $p = 0.0148$; 0–8 h, 113.6 ± 7.45% for control and 142.0 ± 10.48% for netrin treated, $p = 0.0329$; 0–24 h, 117.3 + 9.10% for control and 155.6 ± 11.74% for netrin treated, $p = 0.016$; GFP-syb clusters/branch, 0–4 h, 95.3 ± 7.98% for control and 145.1 ± 13.76% for netrin treated, $p = 0.0032$; 0–8 h, 117.2 ± 9.04% for control, 153.6 ± 10.86% for netrin treated, $p = 0.0163$) (Fig. 4*D*,*E*). That netrin treatment increased branch number but not overall growth, as revealed by the similar increase in axon length in controls and netrin-treated tadpoles, suggests that, on average, individual branches in netrin-treated arbors are shorter in length. Indeed, a measure of average axon segment length indicates that netrin treatment reduced the length of each branch relative to controls (arbor length/branch number: 8–24 h, 107.7 ± 4.37% for control; 95.66 ± 3.30% for netrin treated; $p = 0.0423$) (Fig. 4*F*).

The distribution of DCC immunoreactivity by light microscopy and electron microscopy indicated that, within the retinotectal circuit, the DCC netrin receptor is preferentially localized presynaptically in RGC axons (Fig. 2*J–M*). Microinjection of DCC function-blocking antibodies therefore allowed us to directly assess the effects of tectum-derived netrin on RGC axon branching and the formation of presynaptic specializations. Microinjection of DCC function-blocking antibodies resulted in a smaller increase in the absolute number of GFP-synaptobrevin presynaptic sites relative to controls by 8 h after treatment (0–8 h, 21.47 ± 5.857 for control and 6.364 ± 5.030 for anti-DCC treated; $p = 0.0744$), an observation that became statistically significant by the end of the observation period (0–24 h, 46.53 ± 8.129 for control and 4.091 ± 9.034 for anti-DCC treated; $p = 0.002$) (Fig. 3*B*). In fact, the total number of GFP-synaptobrevin presynaptic sites changed very little over the 24 h observation period after blockade of DCC signaling (Fig. 3*A*,*B*).

The increase in the absolute number of branches normally observed in controls was also prevented after microinjection of DCC function-blocking antibodies (Fig. 3*C*). By the 24 h observation time point, the net increase in branch number was lower in the tadpoles treated with anti-DCC relative to controls, although values did not reach significance (0–24 h, 13.00 ± 3.299 for control and 4.917 ± 2.848; $p = 0.084$). When these effects were examined as a percentage of change relative to the entire arbor at time 0 h, however, blocking DCC function resulted in the failure of axons to increase the total presynaptic site and branch number at a rate similar to controls from 8 h onward (total presynaptic sites: 0–8 h, 139.0 ± 9.53% for control and 102.9 ± 6.39% for anti-DCC treated, $p = 0.0129$; 0–24 h, 193.8 ± 18.74% for control and 99.67 ± 11.52% for anti-DCC treated, $p = 0.0015$; total branch number: 0–8 h, 112.5 ± 4.74% for control and 99.95 ± 4.12% for anti-DCC treated, $p = 0.0722$; 0–24 h, 142.5 ± 7.27% for control and 115.4 ± 9.81% for anti-DCC treated, $p = 0.032$) (Fig. 4*A*,*B*). Although addition of recombinant netrin did not affect axon arbor length, blocking DCC signaling prevented the normal axon arbor growth observed in controls (0–24 h, 169.0 ± 9.05% for control and 123.9 ± 4.87% for anti-DCC treated; $p = 0.0013$) (Fig. 4*C*), suggesting that DCC-mediated netrin signaling is required for the overall differentiation of retinal axons at their target. Importantly, presynaptic site density was also reduced by the end of the 24 h observation period (GFP-syb clusters/length: 0–24 h, 117.3 ± 9.10% for control, and 82.55 ± 9.68% for anti-DCC treated, $p = 0.0193$; GFP-syb clusters/branch: 0–24 h, 128.9 ± 12.85% for control, and 83.09 ± 8.60% for anti-DCC treated, $p = 0.0183$) (Fig. 4*D*,*E*), indicating that blocking DCC function likely has a direct effect on presynaptic specialization in addition to its effect on axon arbor growth and branching.

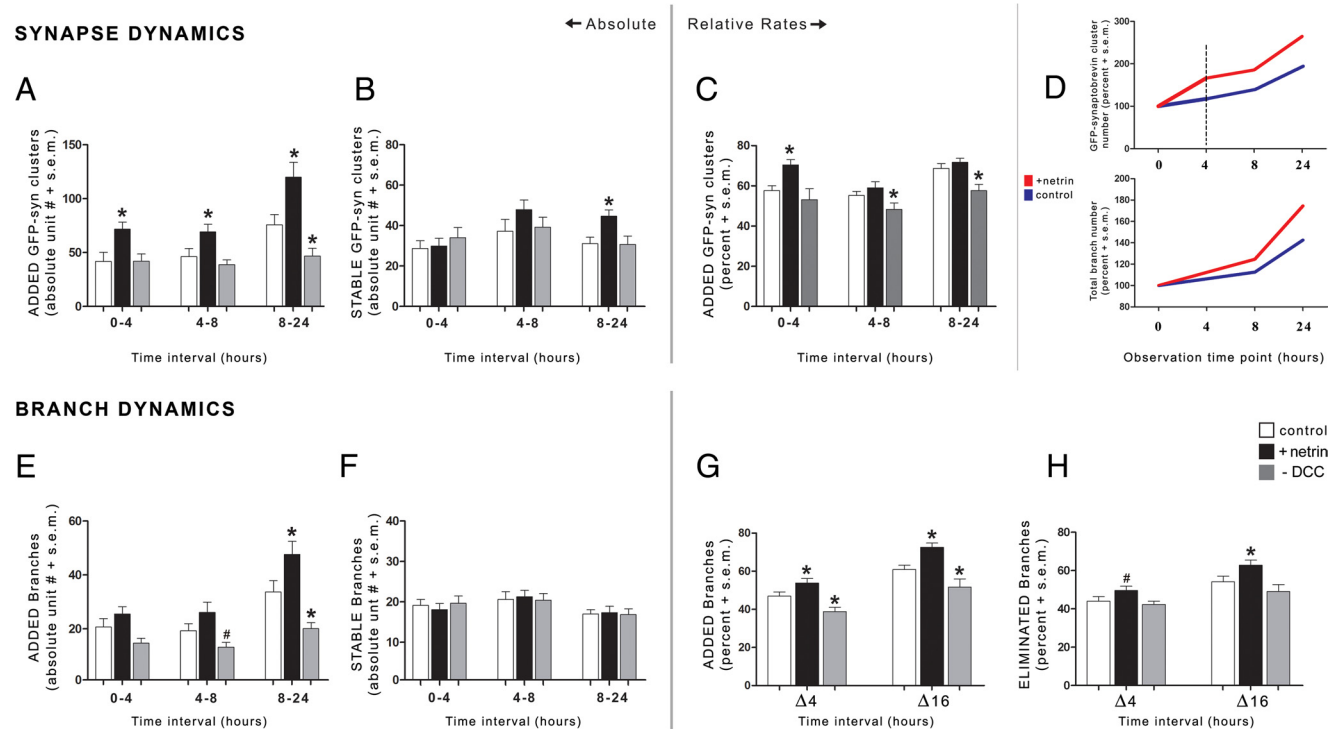

Figure 5. Perturbations in netrin signaling alter presynaptic site and axon branch dynamics. ***A–D***, Netrin and anti-DCC influence presynaptic site dynamics. ***A***, The number of GFP-synaptobrevin-labeled presynaptic sites added was significantly higher in RGCs axons in tadpoles treated with netrin-1 at all observation intervals (*y*-axis; absolute values). The number of newly added GFP-synaptobrevin-labeled presynaptic sites, however, was decreased after anti-DCC treatment, an effect that became significant in the 8–24 h observation interval. ***B***, A small and gradual increase in the number of stabilized presynaptic clusters was observed after netrin treatment, with the number of stabilized presynaptic sites becoming significantly higher than controls in the 8–24 h interval. ***C***, When expressed as percentage of initial value, the number of presynaptic clusters added after netrin treatment was significantly different from controls at the 0–4 h observation interval only. This suggests that the rate of presynaptic cluster addition was rapidly increased after netrin treatment, to then be maintained at a rate that matched controls. In contrast, when compared with its initial value (percentage of total), the number of presynaptic clusters added was significantly lower in RGC axons in anti-DCC-treated tadpoles both at 4–8 and 8–24 h when compared with controls. Anti-DCC had no effect, however, on the number of GFP-synaptobrevin clusters stabilized (***B***). ***D***, The rates of increase in total presynaptic site (top), and branch number (bottom), in RGC axons treated with netrin (red) relative to controls (green) are also illustrated by the line graphs. ***E–H***, Netrin and DCC influence branch addition but not stabilization. ***E***, Netrin-1 increased the number of branches added throughout the imaging period, an effect that was significant from 8 to 24 h. The number of branches added in RGC axons in tadpoles treated with anti-DCC, in contrast, was significantly lower at the 8–24 h observation interval when compared with controls. ***F***, Netrin and anti-DCC did not alter the number of branches stabilized. ***G***, ***H***, The rates of branch addition (***G***), and elimination (***H***), were significantly higher at all observation intervals after netrin treatment and, conversely, the rates of branch addition were significantly lower after anti-DCC treatment when compared with controls (Δ4 h: 0–4 h, 4–8 h data combined). Anti-DCC did not affect the rate of branch elimination (***H***). *Significance with $p \leq 0.05$. #Trend toward significance with $0.05 > p < 0.10$. Error bars indicate SEM.

Microinjection of recombinant netrin-1 induced presynaptic site addition and stabilization and more dynamic branching behavior in retinal axons

Determining changes in the total number of branches and presynaptic sites establishes whether a particular manipulation can alter the complexity of an axon arbor and its synapse density. However, this does not provide insight into whether these changes result from an effect on the genesis of branches and synapses, or whether there has been a change in the ability of synapses and/or branches to stabilize. Here, we analyzed the effects of altering netrin signaling on the addition and stability of branches and GFP-synaptobrevin-labeled presynaptic sites by examining their dynamics. The fate of every branch and presynaptic site within an axon arbor was followed from one observation time point to the next (0 h→4 h; 4 h→8 h; and 8 h→24 h) (see Materials and Methods) to determine the rates of branch and presynaptic site addition and stabilization.

Microinjection of recombinant netrin-1 produced an increase in the absolute number of new GFP-synaptobrevin clusters that were added by the end of the first observation period (0–4 h, 41.87 ± 8.505 for control and 71.64 ± 6.714 for netrin treated; $p = 0.0161$), an effect that persisted for every subsequent observation interval throughout the 24 h period (4–8 h, 46.13 ± 7.534 for control and 69.18 ± 7.102 for netrin treated, $p = 0.0416$; 8–24 h, 75.67 ± 9.469 for control and 119.9 ± 13.81 for netrin treated, $p = 0.0115$) (Fig. 5*A*). Concomitant with this, a tendency toward increased stabilization was observed between 4 and 8 h, and a significant and robust, close to 50% increase in the absolute number of stabilized presynaptic sites was observed from 8 to 24 h (8–24 h, 31.13 ± 3.094 for control and 44.64 ± 3.099 for netrin treated; $p = 0.0061$) (Fig. 5*B*).

Microinjection of netrin-1 also induced changes in the absolute number of branches that were added. Notably, these effects were more gradual, occurring later in the 24 h observation period. A significant increase in the number of branches added was induced between 8 and 24 h (33.69 ± 4.25 for control and 47.64 ± 4.85 for netrin treated; $p = 0.0386$) (Fig. 5*E*), whereas a trend was observed during the first two shorter observation time intervals (0–4 h; 4–8 h). The absolute number of stabilized branches, however, remained very similar to controls across all observation time intervals (Fig. 5*F*). This suggests that the number of branch extensions in the netrin-treated tadpoles that exceed that of controls tend to be less stable. Thus, unlike its effects on presynaptic sites, netrin-1 does not appear to contribute to branch stabilization. Furthermore, this suggests that netrin treatment truly leads to increased dynamic branching behavior, with increased branch additions and branch eliminations.

To further determine the impact of increased presynaptic site addition to the overall synaptic complexity of RGC axons, we quantified GFP-synaptobrevin cluster addition and expressed it as the percentage of newly added presynaptic sites relative to the total presynaptic site number of the axon at the end of each observation period (0–4, 4–8, 8–24 h) (Fig. 5*C*). Microinjection of netrin-1 induced a significant increase in the relative number of GFP-synaptobrevin clusters added during the first 4 h after treatment (0–4 h, 57.63 ± 2.399% for control and 70.45 ± 2.556% for netrin treated; $p = 0.0014$) (Fig. 5*C*). The relative number of GFP-synaptobrevin presynaptic sites added after netrin treatment, however, was not significantly different from controls at the 4–8 and 8–24 h observation intervals when expressed as percentage of total (Fig. 5*C*), whereas the net number of presynaptic sites added was significantly higher than controls (Fig. 5*A*). An interpretation of these results is that, after an initial sharp increase in presynaptic site number during the first 4 h after treatment (Fig. 5*A*), the synaptically more complex netrin-treated arbors required a greater number of new presynaptic sites to be added to continue to differentiate at a rate comparable with that of controls for the remainder of the observation period (4–8 and 8–24 h) (Fig. 5*C*). The requirement for a higher net number of presynaptic sites added after an initial increase in presynaptic site differentiation is better exemplified in Figure 5*D*. The slope of the line graph represents the rate of increase in total presynaptic site number over the 24 h observation period. The steeper part of the slope illustrates an increase in growth rate from 0 to 4 h, and its subsequent angle change represents a similar rate of presynaptic growth from 4 to 24 h in RGC axons in the netrin-treated tadpoles relative to controls (Fig. 5*D*). Thus, the relative increase in presynaptic site number produced between 0 and 4 h is maintained for the remainder of the 24 h observation period (Figs. 6, 7).

A similar analysis of rates of branch addition, expressed as percentage of total, shows that the effects of netrin treatment on axon branching were more gradual (Fig. 5*G*) (also Fig. 5*D*). Dynamic axon branching behavior was increased in the netrin-treated tadpoles at all observation intervals (Fig. 5*G*), with a small but significant increase in the rate of branch additions occurring every 4 h for the first 8 h (Δ4 h, 46.90 ± 2.182% for control and 53.84 ± 2.362% for netrin treated; $p = 0.0349$), as well as in the last observation interval (8–24 h, 63.06 ± 2.092% for control and 72.29 ± 3.249% for netrin treated; $p = 0.0082$). When analyzed in a similar manner, more branches were eliminated after netrin treatment, an effect that was significant only in the last observation interval (Δ4 h, 44.02 ± 2.387% for controls and 49.55 ± 2.297% for netrin treated, $p = 0.095$; 8–24 h, 54.18 ± 2.925% for control and 62.81 ± 2.648% for netrin treated, $p = 0.0405$) (Fig. 5*H*). The contribution of increased branch addition and elimination rates in response to netrin treatment therefore translates into modest step increases in total branch number and thus a significantly more branched arbor by the end of the 24 h observation period (Fig. 4*B*) (also Figs. 6, 7).

Blockade of DCC-mediated netrin signaling prevents RGC axon arbor growth by altering presynaptic site and axon branch addition

As illustrated in Figure 4, blocking DCC signaling prevented normal axon arbor growth 24 h after microinjection of DCC function-blocking antibodies (also Figs. 6, 7). Analysis of presynaptic site and branch dynamics revealed that the effects of anti-DCC treatment were the result of fewer presynaptic sites and axon branches being added during the last observation interval (8–24 h, presynaptic sites, 75.67 ± 9.469 in control and 46.64 ± 7.258 in anti-DCC; $p = 0.0316$) (Fig. 5*A*) (branches, 33.69 ± 4.246 for control and 20.08 ± 2.19 for anti-DCC; $p = 0.0161$) (Fig. 5*E*). The stability of both presynaptic sites (Fig. 5*B*) and branches (Fig. 5*F*), however, were similar to controls at all observation intervals. When changes were measured relative to the initial complexity of the axons, presynaptic site addition was significantly decreased during the second observation interval from 4 to 8 h and this effect persisted for the remainder of the 24 h observation period (4–8 h, 55.27 ± 2.00% in control and 47.27 ± 3.19% after anti-DCC treatment, $p = 0.050$; 8–24 h, 68.73 ± 2.35% in control and 57.64 ± 3.14% in anti-DCC, $p = 0.0081$) (Fig. 5*C*). Consistent with a role for DCC-mediated netrin signaling in axon branching, anti-DCC treatment decreased the rates of branch addition when compared with controls at all observation intervals (branch additions, Δ4 h, 46.90 ± 2.182% for control and 38.80 ± 2.332% for anti-DCC, $p = 0.0145$; 8–24 h, 60.90 ± 2.235% for control and 51.67 ± 4.281% for anti-DCC, $p = 0.0485$) (Fig. 5*G*). The rates of branch elimination, however, were unchanged (Fig. 5*H*). These data indicate that the absence of DCC-mediated netrin signaling affects presynaptic site differentiation and branch extension without compromising the stability of existing synapses and branches.

Discussion

Although a growing number of molecules are being identified as factors that influence axon branching and synaptogenesis, very few specific cues have been examined in a real-time *in vivo* context to determine their impact on arbor dynamics. Here, we identify netrin as an important mediator of RGC axon branching and synaptogenesis in the developing *Xenopus* retinotectal system. Microinjection of netrin-1 resulted in the differentiation of axon arbors with a higher density of GFP-synaptobrevin-labeled presynaptic sites that became morphologically more complex than controls over time. The effect of netrin on synapses was the result of a rapid increase in presynaptic site additions that persisted for the duration of the 24 h posttreatment observation period, along with a gradual increase in the net number of stabilized presynaptic sites. The increase in presynaptic site differentiation induced by netrin treatment was followed by a gradual increase in dynamic branching behavior, determined by an increase in branch extensions and retractions without any accompanying increase in the number of stable branches. This suggests that newly formed branches induced by the netrin treatment are less likely to stabilize. This dynamic branching eventually led to a more complex arbor because of a greater increase in the rate of branch extensions relative to the number of branches lost during the final observation interval.

In the developing retinotectal circuit, DCC was found to be expressed by RGCs when their axons are terminating and branching in the optic tectum. Inhibition of DCC signaling confirmed that netrin influences the differentiation program of RGC axons. Axon arbors in anti-DCC-treated tadpoles were less dynamic, adding fewer presynaptic sites and fewer branches during a 24 h observation period. The absolute number of stabilized presynaptic sites and branches was unchanged relative to controls, indicating that loss of DCC function does not affect the stability of existing branches and presynaptic sites. Consistent with this observation, RGC axon arbor morphology and complexity changed very little over the 24 h observation period. Together, these data indicate that DCC-mediated netrin signaling is required for RGC axon differentiation and that netrin impacts on presynaptic site differentiation and axon branch extension.

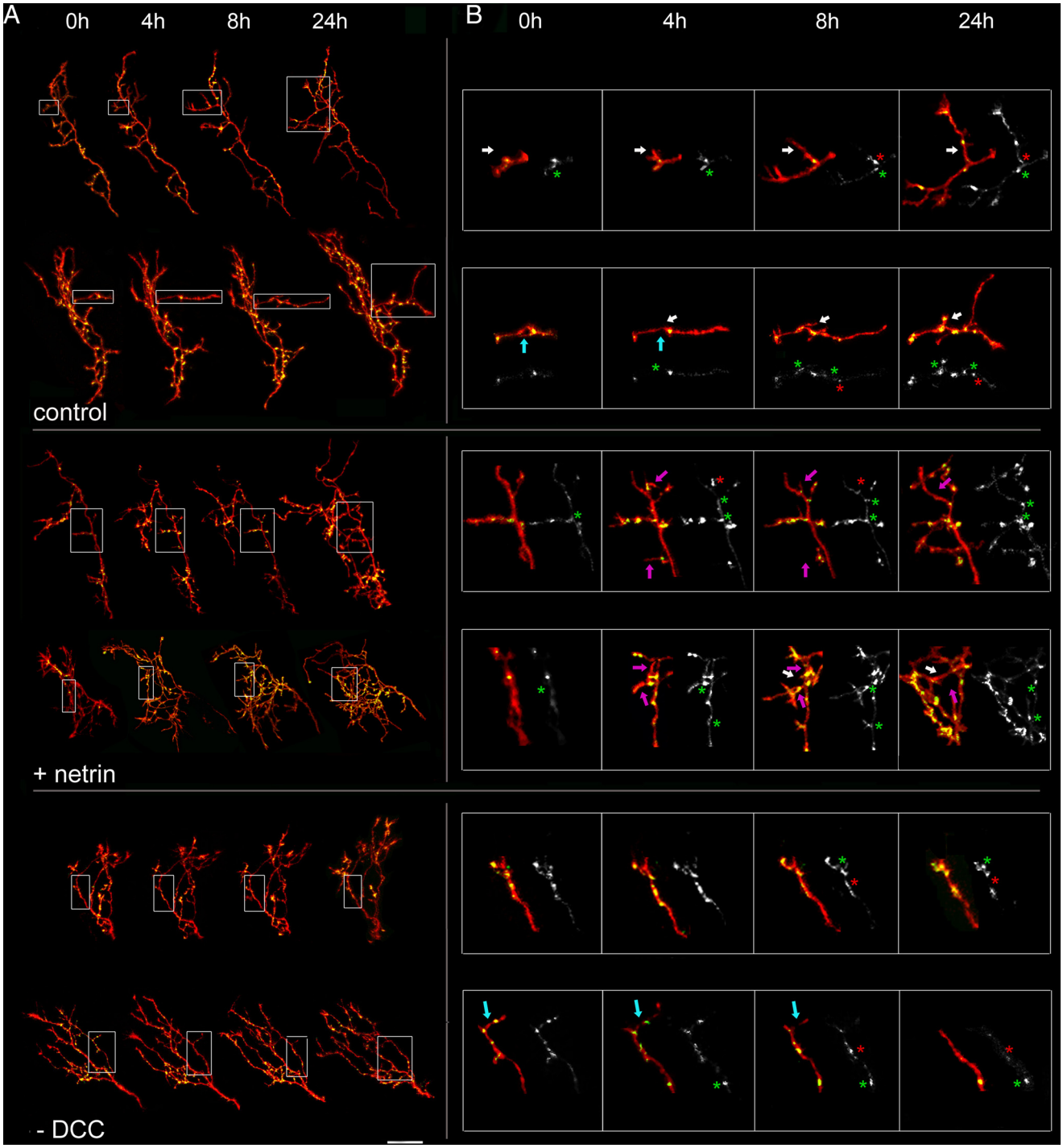

Figure 6. Dynamic changes in presynaptic structure in RGC axon arbors in response to alterations in netrin signaling. ***A***, Confocal projections of representative RGC axons coexpressing Ds-Red (red) and GFP-synaptobrevin (green) in tadpoles microinjected with netrin-1 (+ netrin) or DCC function-blocking antibodies (− DCC) right after the first imaging session. Note the significantly higher number of GFP-synaptobrevin-labeled presynaptic sites in the morphologically more complex arbors after netrin treatment. In contrast, the RGC axon arbors that received anti-DCC treatment did not change their morphology or presynaptic connectivity significantly within a 24 h period (Fig. 7). Scale bar, 50 μm. ***B***, Enlarged projections of single branches for the sample control-, netrin-, and anti-DCC-treated axons shown in ***A*** (gray boxes) illustrate branch and presynaptic site dynamics. Sample branches that were added (white arrows), eliminated (blue arrows), or added and then eliminated (magenta arrows) are shown for each experimental group. More branches were added and then eliminated (magenta arrows) in RGC arbors of netrin-treated tadpoles compared with controls. Although fewer in number, newly added branches in controls tended to remain stable for the remainder of the observation period (white arrows). Preexisting branches were eliminated (blue arrows) after anti-DCC treatment, whereas no new branches were added during the 24 h observation period. Sample GFP-synaptobrevin puncta added (green asterisks) or eliminated (red asterisks) highlight presynaptic site dynamics in the individual axon branches. Note that more GFP-synaptobrevin puncta were added per axon branch within the first 4 h after netrin treatment, and then the number continued to increase more gradually during the remainder of the 24 h observation period. Here, the green asterisks highlight a few examples. In comparison, axon branches in control-treated tadpoles underwent a slower increase in the number of GFP-synaptobrevin puncta across time points, whereas axons added fewer GFP-synaptobrevin puncta after anti-DCC treatment relative to controls. The relative rate of disassembly of GFP-synaptobrevin puncta (red asterisks) in axon branches was similar to controls for both netrin and anti-DCC-treated tadpoles.

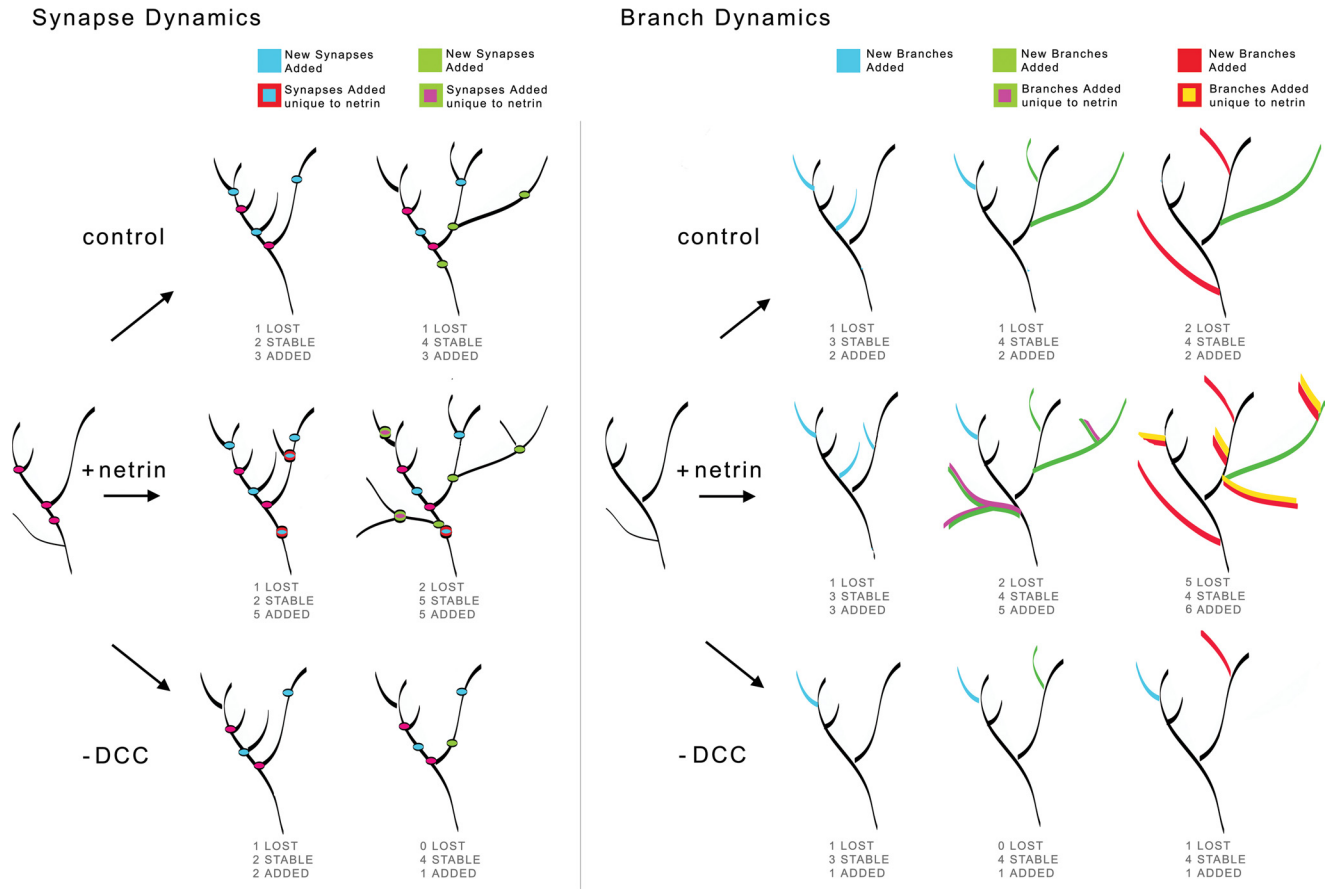

Figure 7. Schematic representation of changes in presynaptic differentiation of RGC axon arbors induced by alterations in DCC-mediated netrin signaling. Top, Control, RGC axons become more complex over time by the dynamic addition, elimination, and stabilization of presynaptic sites (Synapse Dynamics) and axon branches (Branch Dynamics). As more branches are added than eliminated, the arbor gradually increases its complexity over time. Middle, + netrin, Excess netrin induces rapid, novel presynaptic site addition, which gradually results in more stabilized presynaptic sites. The effects of netrin on presynaptic site addition are followed by new branch additions with a time delay. Note that, even though RGC axons exposed to netrin add more new branches, the relative number of branches that are stabilized remains constant. Bottom, − DCC, In contrast to netrin, anti-DCC prevents normal presynaptic addition without influencing presynaptic site stabilization (compare with axon projections shown in Fig. 6). Similarly, blockade of DCC signaling interferes with new branch addition without affecting branch stabilization. Thus, altering DCC-mediated netrin signaling interferes with the normal morphological and synaptic maturation of RGC axon arbors by preventing growth rather than by influencing their stability overall.

Presentation of cues affects function

Molecules that can promote or inhibit growth can function as guidance cues based on the manner in which they are presented. Morphogens, growth factors, and guidance cues have all been shown to direct growth when presented as a gradient (Arévalo and Chao, 2005; Charron and Tessier-Lavigne, 2005). Indeed, how netrin is distributed and presented to the responding cell appears to be an important factor in determining the effects it will exert. There are numerous examples in which netrin functions as a short-range or contact-mediated cue rather than as a long-range axon guidance cue with a graded distribution. In these instances, netrin has contributed to mediating directional changes at an intermediate choice point, such as in RGC axons exiting the retina (Deiner et al., 1997; Höpker et al., 1999), cell–cell interactions in the development of peripheral tissues (Srinivasan et al., 2003; Lu et al., 2004; Park et al., 2004), and in invertebrate synaptogenesis (Winberg et al., 1998; Colón-Ramos et al., 2007). In these short-range functions, netrin is present not as a gradient but in a very discreet pattern in specific cell types. For example, netrin is present in a ring of neuroepithelial cells around the optic nerve head in the retina, and although it functions as an intermediate choice point for navigating RGC axons about to exit the retina, it does not contribute to their guidance to the optic nerve head (Deiner et al., 1997).

Our *in vivo* studies indicate that netrin signaling in actively branching RGC arbors influences presynaptic site differentiation and that this event precedes an effect on axon branch elaboration. In *Drosophila*, netrin has been shown to play a modulatory role at the nerve–muscle synapse in which target-derived netrin and semaphorin regulate, in opposite directions, the number of synapses that will form without actually mediating guidance to the muscles (Winberg et al., 1998). In *C. elegans*, UNC-6/netrin functions as a short-range cue in which the UNC-6/netrin-expressing ventral cephalic sheath cells delimit the area in which presynaptic specializations will form and in which UNC-40/DCC will localize (Colón-Ramos et al., 2007). These findings suggest that our dynamic *in vivo* observations of netrin-mediated effects on presynaptic specialization may involve netrin function as a short-range or contact-mediated cue. Netrin-1 mRNA is expressed in the *Xenopus* optic tectum early during retinotectal development near the ventricle in which putative neuronal precursor cells are born and differentiate (stage 39) (Shewan et al., 2002). Thus, tectal neurons would be capable of expressing and releasing netrin protein as RGC axons first innervate the optic tectum and begin to arborize. Our characterization of netrin protein distribution in the target optic tectum and at putative postsynaptic sites during later stages of RGC axon differentiation (stage 45) suggests a potential mechanism in which axons in

the vicinity of, or making contact with, netrin-expressing tectal neurons will undergo presynaptic specialization at this specific site of interaction. The localization of DCC immunoreactivity at ultrastructurally identified presynaptic sites in the tectal neuropil supports this idea.

Our results show that netrin rapidly influences presynaptic specialization. However, an effect on total branch number was more gradual, with a significantly more exuberant arbor being present only by the end of the 24 h observation period. It is important to note, nevertheless, that branch dynamics, determined by the rate of branch extension and elimination, increased within 4 h after treatment. Thus, the increase in presynaptic site additions coincided with an increase in dynamic branching behavior. Previous *in vivo* time-lapse studies have shown that new branches commonly extend out from an area on the axon that contains a presynaptic specialization (Alsina et al., 2001; Hu et al., 2005). Studies also suggest that the presence of presynaptic specializations on a branch is closely linked to its stability (Meyer and Smith, 2006). It is not clear whether these findings represent a role of presynaptic sites in simply determining the site of a new branch extension or if their presence in fact promotes the formation of a nascent branch and/or its stabilization. Our findings support the possibility that the rapid and dramatic increase in presynaptic site additions may indeed have promoted the new branch extensions that we observed, but that an additional or alternative signal may be necessary for their stabilization.

Multiple dynamic strategies for influencing axon arbor differentiation

New insights into the mechanisms underlying axon arbor differentiation have been obtained through studies that analyze the dynamic behavior of axons in the retinotectal projection of both *Xenopus* and zebrafish embryos (Cohen-Cory, 2002; Hua and Smith, 2004; Niell and Smith, 2004). As the number of specific cues examined grows, it is becoming increasingly apparent that multiple dynamic strategies exist to bring about changes in arbor complexity and synapse density. In addition to the present results, the effects of specific neurotrophic factors, repellent cues, and activity-regulated genes on axon dynamics have been directly examined, and all have been reported to have their own unique dynamic differentiation profile (Cantallops et al., 2000; Alsina et al., 2001; Hu et al., 2005; Javaherian and Cline, 2005; Campbell et al., 2007).

Of particular interest is the comparison between the neurotrophin BDNF and netrin because both cues produce a more complex axon arbor with increased synapse density and they share many common signaling mechanisms (Caroni, 1998; Meyer-Franke et al., 1998; Ming et al., 1999, 2002; Nishiyama et al., 2003; Guirland et al., 2004; Jin et al., 2005; Shim et al., 2005; Wang and Poo, 2005), but the changes in axon dynamics they produce are significantly different. BDNF exerts rapid and significant effects on the addition and stability of presynaptic sites and axon branches (within 2 h of treatment). The dynamics underlying the BDNF-mediated effects involve an increase in synapse density in the longer, more complex arbors (Cohen-Cory and Fraser, 1995; Alsina et al., 2001). Thus, BDNF contributes not only to presynaptic site and branch addition, but there is a significant synapse and branch stabilization component to its function (Cohen-Cory and Fraser, 1995; Hu et al., 2005). Our combined observations with altering netrin levels and DCC signaling indicate that netrin influences first the presynaptic maturation of the axon arbor and then induces new branch growth but not its stabilization. Loss of netrin function prevents presynaptic site and new branch addition, but does not affect the stability of existing presynaptic sites or axon branches. Thus, although both BDNF and netrin increase arbor complexity of RGC axon arbors, the dynamics involved in bringing this about are in fact quite different. Netrin promotes presynaptic site differentiation and then branch extension sequentially, and BDNF promotes growth and stabilization of both presynaptic sites and axon branches in the same time frame. These findings therefore demonstrate that different cues can use unique, and perhaps complementary, dynamic strategies to shape developing neural circuits, even in instances when the end results may appear similar and many signaling mechanisms between the two cues are overlapping.

The dynamics involved in responses to slit and CPG15 also illustrate the variety and range of dynamic responses displayed by axons during circuit formation in response to different developmental cues. Normally, with increased arbor complexity, more mature RGC axon arbors begin to slow their growth rate and stabilize. Slit-1, like netrin-1, was originally identified and characterized as an axon guidance molecule that was subsequently identified as a modulator of axon differentiation events that follow pathfinding. Zebrafish embryos with decreased slit-1 signaling undergo a shift in the period of active axon arbor branching and synapse formation to an earlier developmental stage, stabilizing faster (Campbell et al., 2007), thus suggesting a role for slit-1-Robo signaling in preventing arbor maturation. The activity-regulated candidate plasticity gene CPG15 also affects RGC axon arborization. CPG15 influences the process of slowed axon growth rate as arbors mature, and excess CPG15 selectively increases branch stabilization and synaptic maturation (Cantallops et al., 2000). Thus, the effects of slit-1 and CPG15 in arbor maturation again differ from those induced by netrin, as netrin primarily influences presynaptic differentiation and then branch extension, without affecting branch stabilization.

In conclusion, by directly observing the effects of specific molecular cues on branch and synapse dynamics in the developing retinotectal system, our studies highlight the impact that multiple developmental signals can exert on developing axons, and how signals may be integrated and translated into responses that shape neural morphology and connectivity at the target. Our studies thus identify netrin-1 as an active participant in RGC axon presynaptic differentiation, not only as they navigate along their pathway but also at their target.

References

Alsina B, Vu T, Cohen-Cory S (2001) Visualizing synapse formation in arborizing optic axons in vivo: dynamics and modulation by BDNF. Nat Neurosci 4:1093–1101.

Anderson RB, Holt CE (2002) Expression of UNC-5 in the developing *Xenopus* visual system. Mech Dev 118:157–160.

Arévalo JC, Chao MV (2005) Axonal growth: where neurotrophins meet Wnts. Curr Opin Cell Biol 17:112–115.

Campbell DS, Stringham SA, Timm A, Xiao T, Law MY, Baier H, Nonet ML, Chien CB (2007) Slit1a inhibits retinal ganglion cell arborization and synaptogenesis via Robo2-dependent and -independent pathways. Neuron 55:231–245.

Cantallops I, Haas K, Cline HT (2000) Postsynaptic CPG15 promotes synaptic maturation and presynaptic axon arbor elaboration in vivo. Nat Neurosci 3:1004–1011.

Caroni P (1998) Driving the growth cone. Science 281:1465–1466.

Charron F, Tessier-Lavigne M (2005) Novel brain wiring functions for classical morphogens: a role as graded positional cues in axon guidance. Development 132:2251–2262.

Cline HT (1991) Activity-dependent plasticity in the visual systems of frogs and fish. Trends Neurosci 14:104–111.

Cohen-Cory S (2002) The developing synapse: construction and modulation of synaptic structures and circuits. Science 298:770–776.

Cohen-Cory S, Fraser SE (1995) Effects of brain-derived neurotrophic fac-

tor on optic axon branching and remodelling in vivo. Nature 378: 192–196.

Colón-Ramos DA, Margeta MA, Shen K (2007) Glia promote local synaptogenesis through UNC-6 (netrin) signaling in *C. elegans*. Science 318:103–106.

Deiner MS, Kennedy TE, Fazeli A, Serafini T, Tessier-Lavigne M, Sretavan DW (1997) Netrin-1 and DCC mediate axon guidance locally at the optic disc: loss of function leads to optic nerve hypoplasia. Neuron 19:575–589.

de la Torre JR, Höpker VH, Ming GL, Poo MM, Tessier-Lavigne M, Hemmati-Brivanlou A, Holt CE (1997) Turning of retinal growth cones in a netrin-1 gradient mediated by the netrin receptor DCC. Neuron 19:1211–1224.

Dent EW, Tang F, Kalil K (2003) Axon guidance by growth cones and branches: common cytoskeletal and signaling mechanisms. Neuroscientist 9:343–353.

Dent EW, Barnes AM, Tang F, Kalil K (2004) Netrin-1 and semaphorin 3A promote or inhibit cortical axon branching, respectively, by reorganization of the cytoskeleton. J Neurosci 24:3002–3012.

Finger JH, Bronson RT, Harris B, Johnson K, Przyborski SA, Ackerman SL (2002) The netrin 1 receptors Unc5h3 and Dcc are necessary at multiple choice points for the guidance of corticospinal tract axons. J Neurosci 22:10346–10356.

Gallo G, Letourneau PC (2004) Regulation of growth cone actin filaments by guidance cues. J Neurobiol 58:92–102.

Gitai Z, Yu TW, Lundquist EA, Tessier-Lavigne M, Bragmann CI (2003) The netrin receptor UNC-40/DCC stimulates axon attraction and outgrowth through enabled and, in parallel, Rac and UNC-115/AbLIM. Neuron 37: 53–65.

Govek EE, Newey SE, Van Aelst L (2005) The role of the Rho GTPases in neuronal development. Genes Dev 19:1–49.

Grant A, Hoops D, Labelle-Dumais C, Prévost M, Rajabi H, Kolb B, Stewart J, Arvanitogiannis A, Flores C (2007) Netrin-1 receptor-deficient mice show enhanced mesocortical dopamine transmission and blunted behavioural responses to amphetamine. Eur J Neurosci 26:3215–3228.

Guan KL, Rao Y (2003) Signalling mechanisms mediating neuronal responses to guidance cues. Nat Rev Neurosci 4:941–956.

Guirland C, Suzuki S, Kojima M, Lu B, Zheng JQ (2004) Lipid rafts mediate chemotropic guidance of nerve growth cones. Neuron 42:51–62.

Hedgecock EM, Culotti JG, Hall DH (1990) The unc-5, unc-6, and unc-40 genes guide circumferential migrations of pioneer axons and mesodermal cells on the epidermis in *C. elegans*. Neuron 4:61–85.

Holt CE, Garlick N, Cornel E (1990) Lipofection of cDNAs in the embryonic vertebrate central nervous system. Neuron 4:203–214.

Hong K, Hinck L, Nishiyama M, Poo MM, Tessier-Lavigne M, Stein E (1999) A ligand-gated association between cytoplasmic domains of UNC5 and DCC family receptors converts netrin-induced growth cone attraction to repulsion. Cell 97:927–941.

Höpker VH, Shewan D, Tessier-Lavigne M, Poo M, Holt C (1999) Growth-cone attraction to netrin-1 is converted to repulsion by laminin-1. Nature 401:69–73.

Hu B, Nikolakopoulou AM, Cohen-Cory S (2005) BDNF stabilizes synapses and maintains the structural complexity of optic axons in vivo. Development 132:4285–4298.

Hua JY, Smith SJ (2004) Neural activity and the dynamics of central nervous system development. Nat Neurosci 7:327–332.

Javaherian A, Cline HT (2005) Coordinated motor neuron axon growth and neuromuscular synaptogenesis are promoted by CPG15 in vivo. Neuron 45:505–512.

Jin M, Guan CB, Jiang YA, Chen G, Zhao CT, Cui K, Song YQ, Wu CP, Poo MM, Yuan XB (2005) Ca^{2+}-dependent regulation of rho GTPases triggers turning of nerve growth cones. J Neurosci 25:2338–2347.

Kalil K, Dent EW (2005) Touch and go: guidance cues signal to the growth cone cytoskeleton. Curr Opin Neurobiol 15:521–526.

Keleman K, Dickson BJ (2001) Short- and long-range repulsion by the *Drosophila* Unc5 netrin receptor. Neuron 32:605–617.

Kornack DR, Giger RJ (2005) Probing microtubule +TIPs: regulation of axon branching. Curr Opin Neurobiol 15:58–66.

Lim YS, Mallapur S, Kao G, Ren XC, Wadsworth WG (1999) Netrin UNC-6 and the regulation of branching and extension of motoneuron axons from the ventral nerve cord of *Caenorhabditis elegans*. J Neurosci 19:7048–7056.

Lu X, Le Noble F, Yuan L, Jiang Q, De Lafarge B, Sugiyama D, Bréant C, Claes F, De Smet F, Thomas JL, Autiero M, Carmeliet P, Tessier-Lavigne M, Eichmann A (2004) The netrin receptor UNC5B mediates guidance events controlling morphogenesis of the vascular system. Nature 432:179–186.

Manitt C, Thompson KM, Kennedy TE (2004) Developmental shift in expression of netrin receptors in the rat spinal cord: predominance of UNC-5 homologues in adulthood. J Neurosci Res 77:690–700.

Mann F, Harris WA, Holt CE (2004) New views on retinal axon development: a navigation guide. Int J Dev Biol 48:957–964.

Marshak S, Nikolakopoulou AM, Dirks R, Martens GJ, Cohen-Cory S (2007) Cell autonomous TrkB signaling in presynaptic retinal ganglion cells mediates axon arbor growth and synapse maturation during the establishment of retinotectal synaptic connectivity. J Neurosci 27:2444–2456.

Meyer MP, Smith SJ (2006) Evidence from *in vivo* imaging that synaptogenesis guides the growth and branching of axonal arbors by two distinct mechanisms. J Neurosci 26:3604–3614.

Meyer-Franke A, Wilkinson GA, Kruttgen A, Hu M, Munro E, Hanson MG Jr, Reichardt LF, Barres BA (1998) Depolarization and cAMP elevation rapidly recruit TrkB to the plasma membrane of CNS neurons. Neuron 21:681–693.

Ming G, Song H, Berninger B, Inagaki N, Tessier-Lavigne M, Poo M (1999) Phospholipase C-gamma and phosphoinositide 3-kinase mediate cytoplasmic signaling in nerve growth cone guidance. Neuron 23:139–148.

Ming GL, Wong ST, Henley J, Yuan XB, Song HJ, Spitzer NC, Poo MM (2002) Adaptation in the chemotactic guidance of nerve growth cones. Nature 417:411–418.

Niell CM, Smith SJ (2004) Live optical imaging of nervous system development. Annu Rev Physiol 66:771–798.

Niell CM, Meyer MP, Smith SJ (2004) In vivo imaging of synapse formation on a growing dendritic arbor. Nat Neurosci 7:254–260.

Nieuwkoop PD, Faber J (1956) Normal table of *Xenopus laevis*. Amsterdam: Elsevier North Holland.

Nishiyama M, Hoshino A, Tsai L, Henley JR, Goshima Y, Tessier-Lavigne M, Poo MM, Hong K (2003) Cyclic AMP/GMP-dependent modulation of Ca^{2+} channels sets the polarity of nerve growth-cone turning. Nature 423:990–995.

O'Rourke NA, Fraser SE (1990) Dynamic changes in optic fiber terminal arbors lead to retinotopic map formation: an in vivo confocal microscopic study. Neuron 5:159–171.

Park KW, Crouse D, Lee M, Karnik SK, Sorensen LK, Murphy KJ, Kuo CJ, Li DY (2004) The axonal attractant Netrin-1 is an angiogenic factor. Proc Natl Acad Sci U S A 101:16210–16215.

Pierceall WE, Reale MA, Candia AF, Wright CV, Cho KR, Fearon ER (1994) Expression of a homologue of the deleted in colorectal cancer (DCC) gene in the nervous system of developing *Xenopus* embryos. Dev Biol 166:654–665.

Rodríguez JJ, Davies HA, Silva AT, De Souza IE, Peddie CJ, Colyer FM, Lancashire CL, Fine A, Errington ML, Bliss TV, Stewart MG (2005) Long-term potentiation in the rat dentate gyrus is associated with enhanced Arc/Arg3.1 protein expression in spines, dendrites and glia. Eur J Neurosci 21:2384–2396.

Scheiffele P (2003) Cell-cell signaling during synapse formation in the CNS. Annu Rev Neurosci 26:485–508.

Shewan D, Dwivedy A, Anderson R, Holt CE (2002) Age-related changes underlie switch in netrin-1 responsiveness as growth cones advance along visual pathway. Nat Neurosci 5:955–962.

Shim S, Goh EL, Ge S, Sailor K, Yuan JP, Roderick HL, Bootman MD, Worley PF, Song H, Ming GL (2005) XTRPC1-dependent chemotropic guidance of neuronal growth cones. Nat Neurosci 8:730–735.

Srinivasan K, Strickland P, Valdes A, Shin GC, Hinck L (2003) Netrin-1/neogenin interaction stabilizes multipotent progenitor cap cells during mammary gland morphogenesis. Dev Cell 4:371–382.

Tang F, Kalil K (2005) Netrin-1 induces axon branching in developing cortical neurons by frequency-dependent calcium signaling pathways. J Neurosci 25:6702–6715.

Tong J, Killeen M, Steven R, Binns KL, Culotti J, Pawson T (2001) Netrin stimulates tyrosine phosphorylation of the UNC-5 family of netrin receptors and induces Shp2 binding to the RCM cytodomain. J Biol Chem 276:40917–40925.

Wang GX, Poo MM (2005) Requirement of TRPC channels in netrin-1-induced chemotropic turning of nerve growth cones. Nature 434:898–904.

Winberg ML, Mitchell KJ, Goodman CS (1998) Genetic analysis of the mechanisms controlling target selection: complementary and combinatorial functions of netrins, semaphorins, and IgCAMs. Cell 93:581–591.